

Electrospinning of Degradable Elastomeric Nanofibers with Various Morphology and their Interaction with Human Fibroblasts

Erik Borg,^{1,2} Audrey Frenot,¹ Pernilla Walkenström,¹ Katrin Gisselfält,³ Christina Gretzer,³ Paul Gatenholm²

¹IFP Research, Swedish Institute for Fiber and Polymer Research, Mölndal, Sweden

²Department of Material and Surface Chemistry Biopolymer Technology, Chalmers University of Technology, SE 412 96 Göteborg, Sweden

³Artimplant AB, Hulda Mellgrens gata 5, SE-421 32 Västra Frölunda, Sweden

Received 31 January 2007; accepted 26 June 2007

DOI 10.1002/app.27328

Published online 2 January 2008 in Wiley InterScience (www.interscience.wiley.com).

ABSTRACT: Artelon[®] (degradable poly(urethane urea) elastomer) was electrospun into scaffolds for tissue engineering. The diameter of the electrospun fibers, studied by scanning electron microscopy, ranged from 100 nm to a few μm , with an average diameter of 750 nm. The molar mass of the polymer had a major influence on the morphology of the scaffold. Furthermore, aging of the polymer solution caused changes in viscosity, as measured by stress sweeps between 13.5–942 Pa that affected the morphology. The electrospun Artelon mats exhibited about the same elongations to break, both exceeding 200%, measured by

tensile tests. The degradation study showed similar degradation behavior in electrospun mats and solids. *In vitro* study showed that human fibroblasts not only adhere to the surface but also migrate, proliferate, and produce components of an extracellular matrix. These results strongly support the use of electrospun Artelon as a scaffold in tissue engineering. © 2008 Wiley Periodicals, Inc. *J Appl Polym Sci* 108: 491–497, 2008

Key words: electrospun-nanofibers; extensible; degradable; fibroblast; poly(urethane urea)

INTRODUCTION

Tissue engineering is an attractive approach for substituting and/or repairing damaged, resected or malfunctioning tissues and internal organs. In the past years degradable polymers have received greater interest for use in structural scaffolds. In the process of reconstruction of tissue the scaffold should act as an artificial extracellular matrix (ECM) to which the cells can attach and migrate into and start to produce a new natural ECM as the scaffold slowly degrades. A degradable poly(urethane urea), Artelon[®], with elastic properties has recently been introduced on the rapidly growing market segment of orthobiologics. Clinical results show that implants made from Artelon fibers successfully act as scaffolds for tissue engineering in the treatment of thumb base osteoarthritis.¹ Long-term clinical data and biopsy specimens from patients have shown that the material is well tolerated and becomes inte-

grated in the surrounding tissue without causing untoward reactions.

The ECM in the body provides guidance for cell organization, function and survival, and electrospinning is an emerging technique to produce nanofibers that can mimic the fibrillar structure of the ECM. The fiber diameters of the electrospun material are similar to the fiber diameters in the ECM. The pores are interconnected, which is essential for nutrients and waste transport, and the high porosity of the electrospun mats gives a large internal surface area for cell attachment. The morphology, the composition, and the porosity of the electrospun nanofiber mats can also be changed to fit desired applications,^{2–5} and a wide range of different uses have now been proposed for electrospun material in medical applications. Numerous cell studies have also been successfully carried out on electrospun polymers.^{6–20}

Since the pioneering work of Reneker and co-workers^{21,22} it has proven to be possible to electrospin numerous polymers, and a comprehensive list is given in Ref. 23.

Other researchers have reported successful results with electrospinning of other polyurethanes and poly(urethane urea)s, but this is the very first time that the degradable and elastic poly(urethane urea) Artelon has been electrospun. McKee et al.²⁴ prepared electrospun fibrous mats with superior elongation

Correspondence to: P. Walkenström (pernilla.walkenstrom@ifp.se).

Contract grant sponsors: EXPERTISSUES, VINNOVA/IRECO.

from linear and highly branched poly(urethane urea)s. Pedicini and Farris²⁵ reported very different mechanical behavior of electrospun polyurethane as compared with the material from which it was spun. In contrast to the results reported by Mc Kee et al. they saw a decrease in elongation and a stiffer behavior of the electrospun mats. Kihl et al.²⁶ reported that electrospun polyurethane membranes could be useful in improving wound healing. Matsuda and coworkers examined the possibility to simultaneously electrospin segmented polyurethane with other polymers to form multilayered or mixed electrospun mats.² They also manufactured tubular electrospun segmented polyurethane fabrics with different properties.²⁷ Lee et al.⁶ saw that human ligament fibroblasts cultured on aligned polyurethane fibers had a morphology similar to that of ligament fibroblasts *in vivo*. Compared with the nonwoven structure, the aligned structure also led to an increase in ECM production.

The aim of this study was to create nanofibrous nonwoven materials, based on Artelon. The aim was also to use the nanofibrous material as scaffolds and evaluate its morphology, mechanical properties, and degradation kinetics. The interaction between fibroblasts and electrospun Artelon scaffolds was also investigated.

METHODS

Materials

Artelon, a degradable poly(urethane urea), was synthesized in solution by a two-step polymerization method.²⁸ Polycaprolactone (PCL) diol ($M_n = 530$ g/mol) was used as soft segment and 4,4'-diphenylmethane diisocyanate (MDI), 1,3-diaminopropane (1,3-DAP) as hard segment. The solvent used was dimethylformamide (DMF) and the final polymer concentration was 18 wt %. The solutions were either used for electrospinning or cast to films. The films were cast onto glass plates at a uniform thickness of 0.04 mm.

Size exclusion chromatography (SEC) was done with a Waters 2690 Separations Module equipped with a Waters 996 Photodiode Array Detector and a Waters 2410 Refractive Index Detector. Two Styragel columns, HT6E and HT3, were operated in series at a flow rate of 1 mL/min in DMF containing 0.5% (w/v) LiCl to prevent aggregation. The retention times were converted to apparent molar mass using poly(ethylene oxide) standards. The molar mass presented is the peak value and ranged from 125,000 to 144,900 g/mol.

The viscosity of the polymer solutions in DMF was characterized by stress sweeps between 13.5 and 942 Pa at room temperature. The measurements

were made in a Bohlin Rheometer CS 30 (Malvern Instruments, UK) using a cone-and-plate geometry with a diameter of 25 mm and a cone angle of 5.4°.

Electrospinning of Scaffold

The electrospinning set-up used in this study consisted of a grounded metal collector and a power supply connected to a syringe. The power supply was a direct current (DC) high voltage supply from gamma high voltage, USA. The polymer solution was placed in the syringe capped with a 20-G needle. The fibers were spun from an 18 wt % Artelon DMF solution at a voltage of 16 kV, and a grounded aluminum foil was used as a collector. The distance between the nozzle and the collector was 20 cm, and a heat lamp was directed at the spinning set-up to increase the temperature of the environment and, thus, enhance the solvent evaporation and enable collection of dry electrospun fibers. A syringe pump was used to create an even polymer flow of 5.5 mL/h. The shear rate at the wall of the nozzle was calculated to be 57 s^{-1} , using following equation²⁹:

$$\dot{\gamma} = \frac{4Q}{\pi R^3}$$

where Q is the volume flow rate and R the interior radius of the nozzle.

Scaffold Characterization

The morphologies of the electrospun nanofibers were studied by scanning electron microscopy (JSM-T300 (JEOL, Tokyo, Japan)). Prior to examination the samples were sputtered (Fine Coat Ion Sputter JFC-1100 (JEOL, Tokyo, Japan)) with a thin gold layer.

The tensile properties of Artelon samples were determined with a universal test machine (UTM, Instron 1122, manufacture) at a crosshead speed of 5 mm/min equipped with 500-N load cell (according to ASTM 412) at 20°C in 65% relative humidity. The samples dimensions were 10 mm width, 50 mm length, and thicknesses of 0.6 and 0.04 mm for the electrospun mat and reference Artelon film, respectively. The samples were soaked in a 0.9% NaCl-water solution for 5 days prior to the tensile tests. This treatment showed no visible influence on the appearance and dimensions of the samples.

Degradation Test

To investigate the degradation kinetics, samples of solid films and electrospun material were placed in vials in a great surplus of 0.06M phosphate buffer solution pH 7.4.³⁰ The sealed vials were placed in thermostat ovens at 67°C. At intervals the vials were

opened and aliquots of material were taken out. Changes in molar mass were investigated using SEC as described above.

Fibroblast Cell Culturing

The fibroblasts (MRC-5 human fibroblasts at generation 6) (ATCC-Promochem, UK) were cultured to total confluence in culture flasks (Falcon, UK), detached by 0.5% trypsin and EDTA and suspended in complete medium (Dulbeccos Minimum Essential Medium (GIBCO, UK) with 10 vol % supplemented bovine fetal calf serum (GIBCO, UK) and antibiotics (penicillin 50 U/mL and streptomycin 50 µg/mL) to 10^4 cells/mL. Electrospun Artelon scaffolds with a diameter of 8 mm and a thickness of 0.7 mm were sterilized in ethanol (70 vol %) for 1 h, washed in sterile distilled water three times, 10 min each time, and further preconditioned in complete medium for 3 h. The medium was then excluded and the pre-soaked scaffolds were seeded by $\sim 10^4$ cells per scaffold of the cell suspension by direct seeding. The cell-scaffold 3D constructs were cultured for 1, 5, and 8 days. The medium was changed every second day. The study was performed under sterile and static conditions at 37°C in 5% CO₂ and 100% humidity. After the different culture periods the samples were fixated by 2.5% glutaraldehyde in 0.05M sodium-cacodylate pH 7.2, dehydrated in graded series of ethanol, paraffin embedded and sectioned. The sections were routinely stained with hemotoxylin-eosin (Htx-eosin) and for immunocytochemistry. For the immunocytochemistry study, the sections were incubated with biotinylated anticollagen I (Chemicon, US) at a 1 : 100 dilution, followed by avidine : biotinylated enzyme complex (ABC-kit, Vectastain, Vector, US). Finally, the antigen was localized by incubation with 3,3',5,5'-Diaminobenzidine Tetrahydrochloride (DAB), which was used as substrate. The sections were then counterstained with Htx-eosin. The immunocytochemistry evaluations were made in light microscopy using a Nikon Eclipse 50i microscope.

Cell-Scaffold Interactions

Transmission (TEM) and scanning electron microscopy (SEM) evaluations were carried out to investigate cell-scaffold interactions. For SEM, samples were immersion fixated overnight (2% paraformaldehyde and 2.5% glutaraldehyde in 0.05M Na cacodylate buffer) followed by postfixation in 1% OsO₄ for 2 h. Several cycles of exposure to OsO₄ and thiocarbonylhydrazide were also run for postfixation. After dehydration in graded series of ethanol, samples were treated with hexamethyldisilazane and then sputter-coated with a thin (15 nm) Pd layer. All examina-

tions were done in a LEO982 Gemini field emission scanning microscope.

For TEM, samples were first fixated with 2% paraformaldehyde and 2.5% glutaraldehyde in 0.05M Na cacodylate buffer and washed with Na-cacodylate. Postfixation was done with 1% OsO₄ and 1% potassium ferrocyanide in 0.1M Na-cacodylate for 2 h at 4°C, followed by en bloc staining with 1% uranyl acetate in H₂O for 1 h. Specimens were then dehydrated and infiltrated with epoxy resin (Agar 100, Agar Scientific, Stanstead, UK). Semithin sections (0.7 µm) were cut and examined to orientate specimens in the correct way before cutting ultrathin sections (50–60 nm) using a Reichert ultramicrotome equipped with a diamond knife. Sections were contrasted with lead citrate and uranyl acetate before examination in a Zeiss 912AB electron microscope, equipped with a Megaview III camera (SIS, Munster, Germany) and a Proscan TH7896M (Proscan Lagerlefeld, Germany).

RESULTS AND DISCUSSION

Electrospinning of Scaffold

Artelon solutions with different molar masses were successfully electrospun. The electrospun nanofibers were collected as nonwoven mats with dramatically different appearances depending on the molar mass of the polymer [Fig. 1(A,B)]. Higher molar masses gave thicker and smoother fibers [Fig. 1(A)]. At lower molar masses, beads and much thinner fibers were formed [Fig. 1(B)]. The viscosity of Artelon solutions depends on the molar mass of the manufactured polymer. The Artelon solution had higher viscosity at higher molar masses (no figure shown). The viscosity is crucial for the electrospinning process and determines to an extent the appearance of the electrospun material. At higher viscosity, a bimodal fiber diameter distribution is observed [Fig. 1(A)]. Similar phenomenon is also recognized in PEO nanofibers, electrospun from solutions of higher viscosity.²⁶ The driving force for the bead formation is a combination of too low viscous forces and surface tension, which decreases the surface area. At higher viscosities the viscosity prevents the surface tension from inducing beads. Artelon molar masses, M_{peak} , ranging from 125,000 to 134,600 g/mol were successfully electrospun to fibers with diameters in the nanometer range. Higher molar masses, up to 144,900 g/mol, were also successfully electrospun but yielded significantly thicker fibers in the micrometer range.

In addition to the effect of molar mass, the viscosity of the Artelon solutions changes with time. The viscosity measurements in Figure 2 clearly show this aging as a decrease of viscosity and non-Newtonian

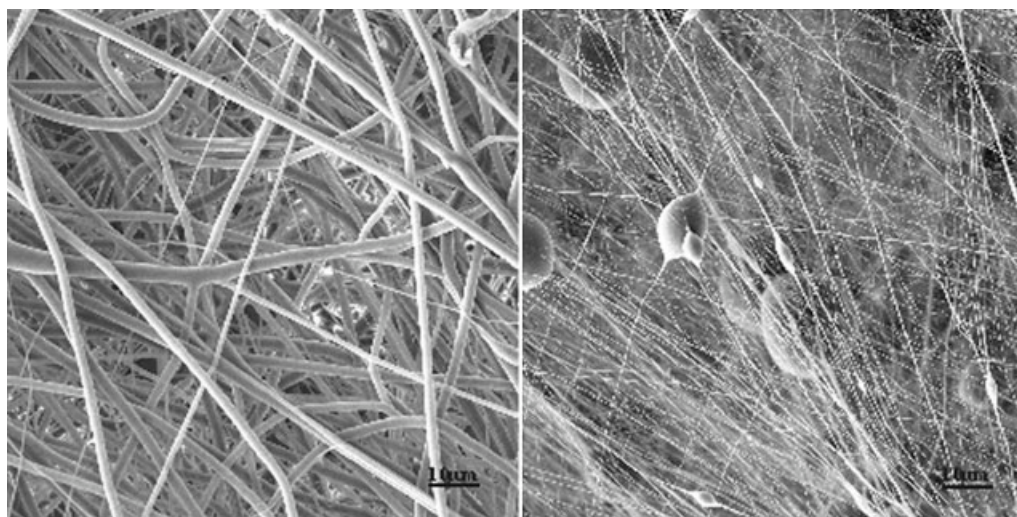


Figure 1 SEM images of Artelon® fibers electrospun from 18 wt % solutions with molar masses of 133,000 g/mol (A) and 127,000 g/mol (B).

behavior of Artelon solutions over the range of shear rates investigated (Fig. 2). Owing to the changes in viscosity with time, the appearance of the subsequently electrospun fibers also changes. Immediately after the fabrication of the polymer solution, and thereby at higher viscosities, smooth fibers and few beads were formed [Fig. 3(A)]. With time and, thus, with a decrease in viscosity, thinner fibers and an increased amount of beads were formed during the electrospinning process [Fig. 3(B,C)]. The behavior corresponds to the results seen when electrospinning different batches with different initial viscosities caused by different molecular weights (Fig. 1).

From the size and weight of the fibrous mats, the porosity of the structure was estimated to be 74% (see the equation below), which is in the same range

as the porosity reported for other electrospun structures.⁶

$$\text{Porosity} = \left(1 - \frac{\text{calculated scaffold density}}{\text{known material density}} \right) \times 100\%$$

Mechanical Properties

Figure 4 shows the typical stress strain relation for solid Artelon films and electrospun Artelon mats with a porosity of 74%. The curves look different at first glance, but the difference in porosity between the materials should be kept in mind. Since stress is calculated as a function of cross section area, material with a porosity of 74% is comparable with a solid divided by a factor of about four. Interestingly the elongations to break are in the same order, both exceeding 200% (Fig. 4). Similar relationships between electrospun mats and solid films have been reported for segmented polyurethane,² but decreased elongation and a stiffer behavior of electrospun polyurethane mats has also been observed.²⁵

Hydrolytic Degradation

The simulated degradation kinetics of electrospun Artelon was compared with that of Artelon films. It was shown that the degradation time was equal for the different forms despite the larger accessible surface in the electrospun material (Fig. 5). The molar mass of both electrospun mats and films seems to increase in the first days after placement in the degradation medium. This is an effect of water uptake, which affects hydrophobic/hydrophilic character of the polymer and thus the solubility of Artelon in

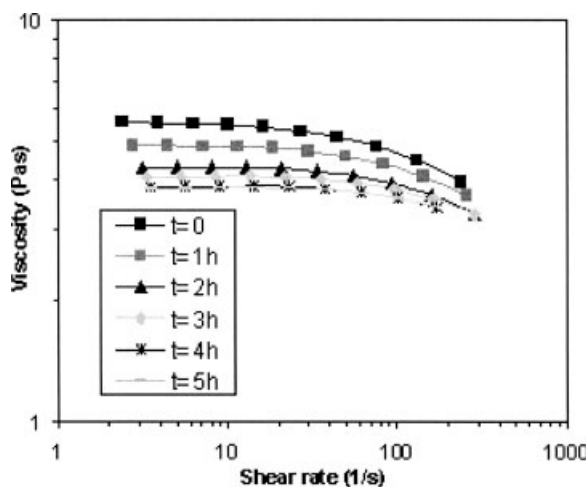


Figure 2 Viscosity-shear rate behavior of Artelon® solutions (18 wt %) at various solution remaining time (t).

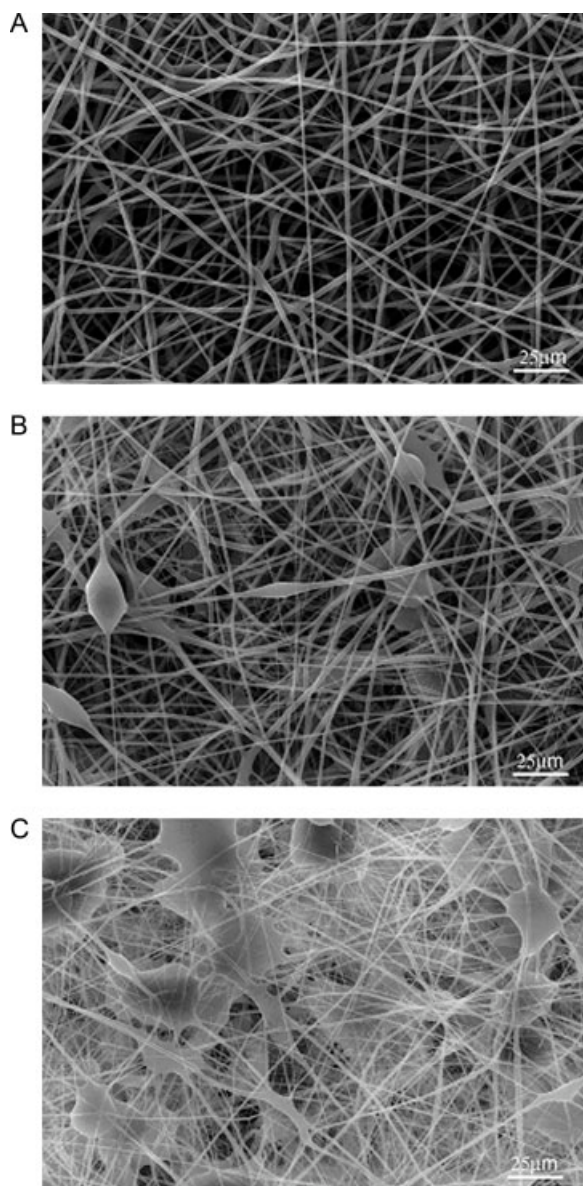


Figure 3 SEM images of Artelon[®] fibers electrospun from an 18 wt % solution at time (t) = 0 h (A); t = 2 h (B) and t = 5 h (C).

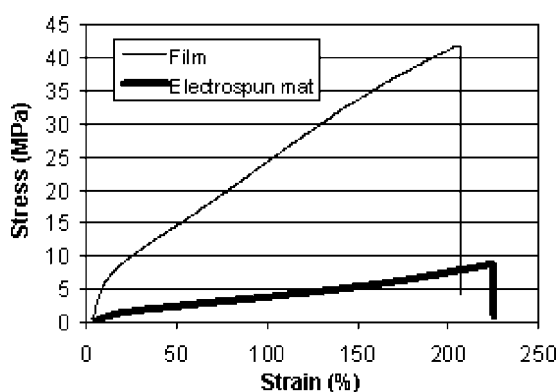


Figure 4 Tensile test results of Artelon[®] films and electrospun Artelon[®] mats.

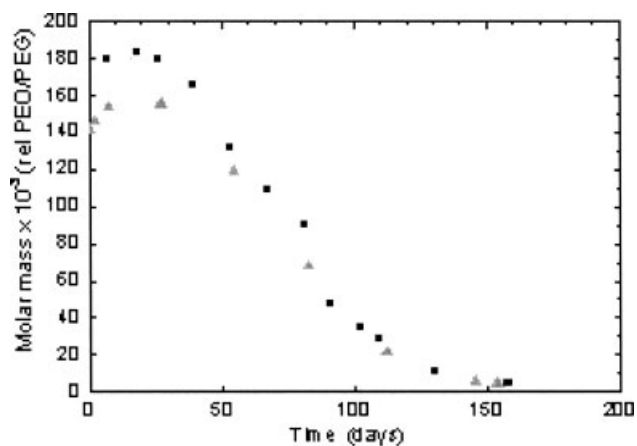


Figure 5 Change in molar mass of Artelon material in phosphate buffer at 67°C. (▲) Electrospun Artelon[®] and (■) Artelon[®] film.

DMF. As SEC is a relative method for measuring molar mass and depends on the solubility of the polymer in a certain solvent this can be seen as an apparent increase in molar mass. The electrospun material has the ability to bind more water than the nonporous film and is therefore affected to a higher degree.

Cell-Scaffold Interactions

The electrospun samples that were seeded with cells were composed of fibers with relatively few beads and a wide diameter distribution, ranging from 100 to 2000 nm, and an average fiber diameter of 750 nm. After 5 days, almost total confluence was detected when cells were cultured on the fiber structure. The Artelon fibers can only partly be detected under the fibroblasts [Fig. 6(A,B)]. The cross section of the electrospun Artelon mat shows a thin layer of fibroblasts on top of the scaffold after 5 days (Fig. 7).

The fibroblasts maintained normal phenotypic morphology in the electrospun Artelon scaffolds examined. This indicates that the cells favor the structure and that they maintain biological functions related to adhesion and migration. As seen in Figure 8, the cells both adhere to the surface and attach mechanically to the scaffold by wrapping pseudopodia around the thin fibers.

Cells cultured on plastic surfaces rapidly lose their differentiated characteristics. To mimic *in vivo* tissue environments, cells can be cultured in different gels or matrices such as collagen and by this can grow in a 3D structure that resembles the *in vivo* architecture.³¹ When culturing in 3D nano structures, such as electrospun Artelon, which mimics the collagen structure of connective tissue, the fibroblasts will have a greater ability to retain their differentiation

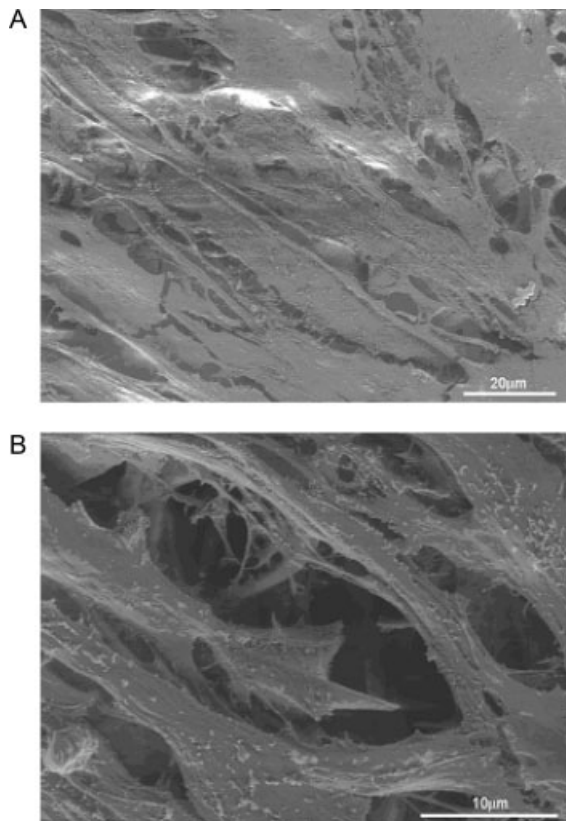


Figure 6 SEM images of Human fibroblasts (MRC-5) cultured *in vitro* on electrospun Artelon[®] for 5 days. SEM image shows cells spread on the fibers and in close contact with the material (A); Fibers can be detected under and between the cells (B).

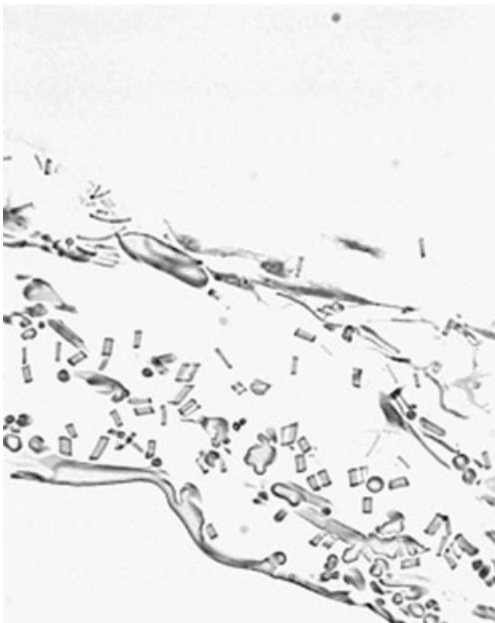


Figure 7 LM images (original magnification $\times 400$) showing cross sections of human fibroblasts (MRC-5) cultured *in vitro* on electrospun Artelon[®] for 5 days. Hematoxylin-eosin staining of a cross section of the cells on top and in between the Artelon[®] fibers.

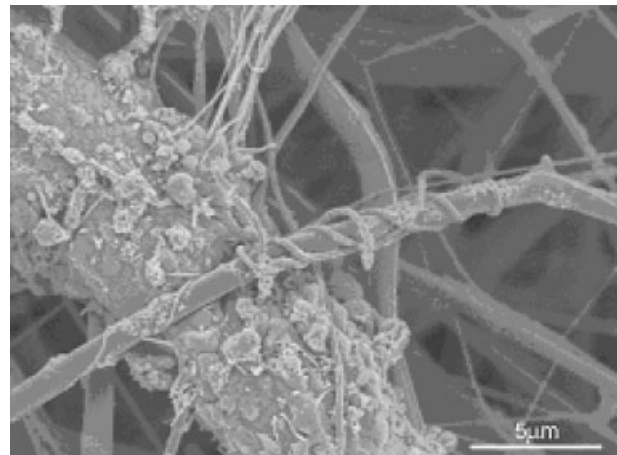


Figure 8 SEM image showing fibroblast (human MRC-5) extension wrapping around the electrospun fiber.

and phenotype characteristics. This has been shown in the *in vitro* models with chondrocytes.³²

The TEM image in Figure 9 shows the close relation between the pseudopodia of fibroblasts and the electrospun Artelon fibers. The interface is probably filled with a protein layer from the outer surface of the cell membrane, showing a close resemblance to cell-cell attachment *in vivo*. The collagen I antibody strongly stains the fibroblasts producing collagen in the electrospun Artelon. The cells are located close to the surface, but some cells are detected within the fibers. All the fibroblasts produce collagen I in the scaffold after 5 days of culture (Fig. 10) and after 8 days (not shown). The collagen I production of the fibroblasts indicates that the cells are active and maintain their important function of producing components of the ECM. New studies are necessary to further investigate the cell-scaffold interactions, in particular the ability of the cells to migrate into the

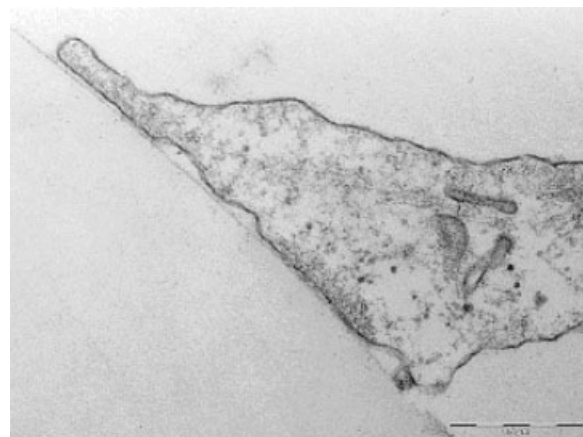


Figure 9 TEM image showing a fibroblast extension in close contact with electrospun Artelon[®].

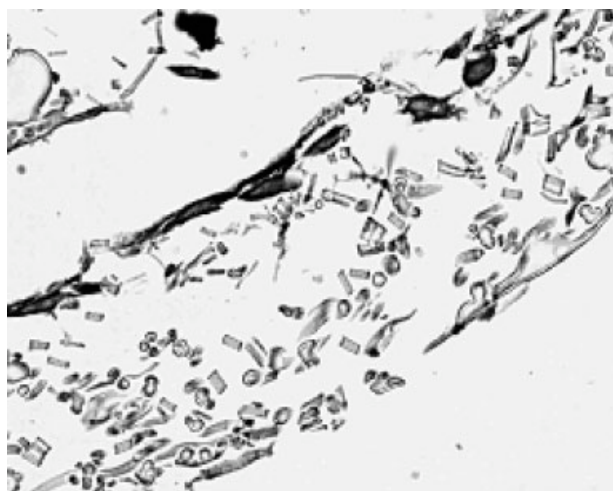


Figure 10 LM-images (original magnification $\times 400$) showing a cross section of human fibroblasts (MRC-5) cultured *in vitro* on electrospun Artelon[®] for 5 days. Immunocytochemical staining for collagen I.

scaffold and the influence of fiber morphology on cell growth.

CONCLUSIONS

In this study, Artelon was electrospun from a DMF solution into fibers with different morphologies for use as scaffold in tissue engineering. The average diameter of the electrospun fibers was around 750 nm, and mechanical tensile strain experiments showed preserved elongation at break compared with the bulk material. The same degradation rate was found for the film and the electrospun mat. In addition to the molar mass dependence of the polymer viscosity, the viscosity also changed with time, leading to different morphologies of the electrospun mats. A favorable interaction between the scaffold and human fibroblasts was demonstrated. Our results indicate that electrospun Artelon may be an excellent candidate as scaffold in tissue engineering.

The authors thank Assoc. Professor Ulf Nannmark, Göteborg University, for his assistance with TEM and SEM images.

References

1. Nilsson, A.; Liljensten, E.; Bergström, C.; Sollerman, C. *J Hand Surg Am* 2005, 30A, 380.
2. Kidoaki, S.; Kwon, I. K.; Matsuda, T. *Biomaterials* 2005, 26, 37.
3. Katta, P.; Alessandro, M.; Ramsier, R. D.; Chase, G. G. *Nano Lett* 2004, 4, 2215.
4. Li, D.; Wang, Y.; Xia, Y. *Adv Mater* 2004, 16, 361.
5. Deitzel, J. M.; Kleinmeyer, J.; Harris, D.; Beck Tan, N. C. *Polymer* 2001, 42, 261.
6. Lee, C. H.; Shin, H. J.; Cho, I. H.; Kang, Y. M.; Kim, I. A.; Park, K. D.; Shin, J. W. *Biomaterials* 2005, 26, 1261.
7. Li, W. L.; Tuli, R.; Okafor, C.; Derfoul, A.; Danielson, K.; Hall, D.; Tuan, R. *Biomaterials* 2005, 26, 599.
8. Ma, Z.; Kotaki, M.; Yong, T.; He, W. *Biomaterials* 2005, 26, 2527.
9. Xu, C. Y.; Inai, R.; Kotaki, M.; Ramakrishna, S. *Biomaterials* 2004, 25, 877.
10. Yang, F.; Murugan, R.; Wang, S.; Ramakrishna, S. *Biomaterials* 2005, 26, 2603.
11. Yoshimoto, H.; Shin, Y. M.; Terai, H.; Vacanti, J. P. *Biomaterials* 2003, 24, 2077.
12. Zong, X.; Bien, H.; Chung, C. Y.; Lihong, Y.; Fang, D.; Hsiao, B.; Chu, B.; Entcheva, E. *Biomaterials* 2005, 26, 5330.
13. Jin, H. J.; Chen, J.; Karageorgiou, V.; Altman, G. H.; Kaplan, D. L. *Biomaterials* 2004, 25, 1039.
14. Min, B. M.; Lee, G.; Kim, S. H.; Nam, Y. S.; Lee, T. S.; Park, W. H. *Biomaterials* 2004, 25, 1289.
15. Mo, X. M.; Xu, C. Y.; Kotaki, M.; Ramakrishna, S. *Biomaterials* 2005, 25, 1883.
16. Min, B. M.; Jeong, L.; Nam, Y. S.; Kim, J. M.; Kim, J. Y.; Park, W. H. *Biol Macromol* 2004, 34, 281.
17. Nair, L. S.; Bhattacharyya, S.; Bender, J. D.; Greish, Y. E.; Brown, P. W.; Allock, H. R.; Laurencin, C. T. *Biomacromolecules* 2004, 5, 2212.
18. Kenawy, E. R.; Layman, J. M.; Watkins, J. R.; Bowlin, G. L.; Matthews, J. A.; Simpson, D. G.; Wnek, G. E. *Biomaterials* 2003, 24, 907.
19. Chua, K. N.; Lim, W. S.; Zhang, P.; Lu, H.; Wen, J.; Ramakrishna, S.; Leong, K. W.; Mao, H. Q. *Biomaterials* 2005, 26, 2537.
20. Kwon, I. K.; Kidoaki, S.; Matsuda, T. *Biomaterials* 2005, 26, 3929.
21. Doshi, J.; Reneker, D. H. *J Electrostat* 1995, 35, 151.
22. Reneker, D. H.; Chun, I. *Nanotechnology* 1996, 7, 216.
23. Huang, Z. M.; Zhang, Y. Z.; Kotaki, M.; Ramakrishna, S. *Compos Sci Technol* 2003, 63, 2223.
24. McKee, M. G.; Park, T.; Unal, S.; Yilgor, I.; Long, T. E. *Polymer* 2005, 46, 2011.
25. Pedicini, A.; Farris, R. *J Polymer* 2003, 44, 6857.
26. Khil, M. S.; Cha, D. I.; Kim, H. Y.; Kim, I. S.; Bhattarai, N. *J Biomed Mater Res* 2003, 67B, 675.
27. Matsuda, T.; Ihara, M.; Inoguchi, H.; Kwon, I. K.; Takamizawa, K.; Kidoaki, S. *J Biomed Mater Res* 2005, 73A, 125.
28. Gisselält, K.; Edberg, B.; Flodin, P. *Biomacromolecules* 2002, 3, 951.
29. Birley, A.; Haworth, B.; Batchelor, J. *Melt flow Properties in Physics of Plastics: Processing; Properties and Materials Engineering*; Hanser: Vienna, 1992; p 59.
30. International Organization for Standardization. *International Standard ISO 13781; 1977 (E)* 1997.
31. Kleinman, H. K.; Graf, J.; Iwamoto, Y.; Kitten, G. T.; Ogle, R. C.; Sasaki, M.; Yamada, Y.; Martin, G. R.; Luckenbill-Edds, L. *Ann N Y Acad Sci* 1987, 513, 134.
32. Malda, J.; van Blitterswijk, C. A.; Grojec, M.; Martens, D. E.; Tramper, J.; Riesle, J. *Tissue Eng* 2003, 9, 939.